ON THE DYNAMICS OF MAXIMIN FLOWS

DRAFT AS OF September 23, 2016

MOODY T. CHU*

Abstract. A flow approach for finding saddle points.

Key words. maximin flow

AMS subject classifications. 65F18, 15A29, 90C52, 68W25,

1. Introduction. The notion of saddle point and the demand for its computation arise from a wide range of disciplines. To demonstrate its importance, we mention two critical applications in practice, namely, the method of Lagrange multipliers for constrained optimization and the dynamical reaction problem.

First, consider the constrained convex programming problem

$$\mathcal{P}: \quad \left\{ \begin{array}{ll} \text{minimize} & \theta(\mathbf{x}) \\ \text{subject to} & g_i(\mathbf{x}) \le 0; \quad i = 1, 2, \ldots, s \\ & g_i(\mathbf{x}) = 0; \quad i = s+1, \ldots, m, \end{array} \right.$$

where the functions $\theta, g_1, \ldots, g_s$ are convex functions mapping from $\mathbb{R}^n$ to $\mathbb{R}$, and $g_{s+1}, \ldots, g_m$ are affine mappings from $\mathbb{R}^n$ to $\mathbb{R}$. Assume that all functions are sufficiently smooth. The Lagrangian L for this problem is the function

$$L(\mathbf{x}, \mathbf{y}) = \theta(\mathbf{x}) + \langle \mathbf{y}, \mathbf{g}(\mathbf{x}) \rangle, \tag{1.1}$$

where entries of $\mathbf{y} \in \mathbb{R}^m$ are the Lagrange multipliers and it is always the case that $y_1, \ldots, y_s$ are nonnegative. Denote $K = \mathbb{R}^s_+ \times \mathbb{R}^{m-s}$. A pair $(\overline{\mathbf{x}}, \overline{\mathbf{y}}) \in \mathbb{R}^n \times K$ is said to be a saddle point for L if the inequalities

$$L(\overline{\mathbf{x}}, \mathbf{y}) \le L(\overline{\mathbf{x}}, \overline{\mathbf{y}}) \le L(\mathbf{x}, \overline{\mathbf{y}}) \tag{1.2}$$

hold for all $(\mathbf{x}, \mathbf{y})$ in a neighborhood of $(\overline{\mathbf{x}}, \overline{\mathbf{y}})$ in $\mathbf{R}^n \times K$. In other words, $\overline{\mathbf{x}}$ minimizes the function $L(\mathbf{x}, \overline{\mathbf{y}})$ among $\mathbf{x}$ and $\overline{\mathbf{y}}$ maximizes $L(\overline{\mathbf{x}}, \mathbf{y})$ among $\mathbf{y}$. The following theorem serves as the basic principle that relates the saddle point of the Lagrangian L to the solution of the primal problem $\mathcal{P}$ [7, 26].

THEOREM 1.1. *(Saddle Point Theorem). Let $\overline{\mathbf{x}} \in \mathbb{R}^n$. If there exists $\overline{\mathbf{y}} \in K$ such that $(\overline{\mathbf{x}}, \overline{\mathbf{y}})$ is a saddle point for the Lagrangian L, then $\overline{\mathbf{x}}$ solves $\mathcal{P}$. Conversely, if $\overline{\mathbf{x}}$ is a solution to $\mathcal{P}$ at which the Slater's constraint qualification is satisfied, then there is a $\overline{\mathbf{y}} \in K$ such that $(\overline{\mathbf{x}}, \overline{\mathbf{y}})$ is a saddle point for L.*

We further know of the following maximin theorem which allows us to interchange the order where $\inf$ and $\sup$ are taken and serves as a basis for the convex duality theory.

THEOREM 1.2. *(Maximin Theorem) If a saddle point for L does exist over $\mathbb{R}^n \times K$, then*

$$\sup_{\mathbf{y} \in K} \inf_{\mathbf{x} \in \mathbb{R}^n} L(\mathbf{x}, \mathbf{y}) = \inf_{\mathbf{x} \in \mathbb{R}^n} \sup_{\mathbf{y} \in K} L(\mathbf{x}, \mathbf{y}) \tag{1.3}$$

Many optimization tactics have been developed in the literature for solving the optimization problem $\mathcal{P}$, which will not be elaborated in this paper. We simply want to point out the mathematical connection between a solution to the primal problem $\mathcal{P}$ and a saddle point to the Lagrangian L.

Second, in the reaction dynamics of complex systems, rare but perceptible transition events between long lived states are of fundamental importance. The presence of transition events, the knowledge of their location in the configuration space, and frequency of these incidents provide critical information for important systems such as phase transitions in nucleation, conformational changes in macromolecules, and transition states in

*Department of Mathematics, North Carolina State University, Raleigh, NC 27695-8205. (chu@math.ncsu.edu) This research was supported in part by the National Science Foundation under grants DMS-1014666 and DMS-1316779.

chemical reactions [19]. We illustrate this point by considering the potential energy surface as an example. Suppose that $U(\mathbf{x})$ denotes a potential function in a chemical system, where $\mathbf{x} \in \mathbb{R}^{3n}$ represents the positions of n atoms in the space. A specific configuration of the atoms corresponds uniquely to a specific energy level. In this way, the potential is parameterized in terms of the positions of the nuclei. Stable arrangements of the atoms, observable in the forms of reactants, products, or intermediates in the system, are those configurations which minimize the potential $U(\mathbf{x})$. These metastable states usually can hold for an extended period of time. However, sudden jumps from one state to another state do happen. Suppose that the potential function forms a smooth landscape. Then its minima usually are surrounded by energy barriers. Transition states correspond to saddle points on this surface. Knowing when, where, how these transitions happen is critically important.

For dynamical reaction problems, it is generally assumed that the transition states are of *index one*, that is, the corresponding Hessian at such a stationary point of $U(\mathbf{x})$ has one and only one negative eigenvalue. Most sophisticated numerical techniques developed for finding the transition pathways crossing these transition states are based on this assumption [8, 11, 13, 27, 30, 31]. In contrast, our dynamical system presented in this paper can handle higher-index problems. Finding saddle points having high but unknown index is a much harder problem.

Although the two scenarios described above are all about finding the saddle point, there is one fundamental difference. In the Lagrangian formulation, it is clear that the space variable $\mathbf{x}$ is to be minimized while the Lagrange multipliers $\mathbf{y}$ are to be maximized at the saddle point. The variables $(\mathbf{x}, \mathbf{y})$ are unequivocally separated into two groups each of which has a definitive dimensionality (index n). This kind of specifically oriented, high-indexed problems is the ideal target of our maximin flow approach. In the dynamical reaction setting, however, we generally do not know which variable or collection of variables attributes to the direction of the corresponding eigenvector, even under the assumption that there is one and only one negative eigenvalue of the Hessian at the saddle point. The Müller-Brown potential energy surface, for instance, has two saddle points of index one, but they are of different orientations. Still, our flow can manifest some useful information.

2. Maximin flows. To fix our idea, we shall concentrate on the problem

$$\max_{\mathbf{y}\in\mathbb{R}^m} \min_{\mathbf{x}\in\mathbb{R}^n} f(\mathbf{x}, \mathbf{y}), \tag{2.1}$$

where $f : \mathbb{R}^n \times \mathbb{R}^m \to \mathbb{R}$ is sufficiently smooth. Starting from any initial point, we define a flow $(\mathbf{x}(t), \mathbf{y}(t))$ via the autonomous differential system, referred to as a maximin flow or a saddle-point flow [2, 5],

$$\begin{cases} \frac{d\mathbf{x}}{dt} &= -\frac{\partial f}{\partial \mathbf{x}}, \\ \frac{d\mathbf{y}}{dt} &= \frac{\partial f}{\partial \mathbf{y}}, \end{cases} \tag{2.2}$$

where $\frac{\partial}{\partial \mathbf{x}}$ and $\frac{\partial}{\partial \mathbf{y}}$ represent the parts of the gradient with respect to the variable $\mathbf{x}$ and $\mathbf{y}$, respectively. We mention in passing that if the variables are limited to some feasible set, such as that in Problem (1.1), then a modification by projecting the vector field (2.2) onto the corresponding tangent subspace should be applied.

We quickly point out that the maximin flow (2.2) is function dependent. It is possible that a different description of the very same saddle point will end up with a very different dynamics. For instance, the surfaces in $\mathbb{R}^3$ corresponding to the objective functions $f_1(x, y) = x^2 - y^2$ and $f_2(x, y) = 2xy$ are essentially the same hyperbolic parabolas by a rotation of $\frac{\pi}{4}$. However, the integral curves associated with f_1 and f_2 are semi-arrays pointing to the origin and concentric circles around the origin, respectively. For the later, it should be quite clear that neither order $\max_y \min_x \min_x \max_y$ makes any difference at all.

Our motivation for proposing the dynamical system (2.2) is quite straightforward. Since the objective in (2.1) is a maximin problem, we wish to move $\mathbf{x}$ in such a way to decrease the value of f, when $\mathbf{y}$ is held constant; and move $\mathbf{y}$ to increase the value of f, when $\mathbf{x}$ is kept invariant. In a sense, the differential equation is an infinitesimal version of the classical alternative direction iteration, except that the pair $(\mathbf{x}, \mathbf{y})$ changes simultaneously and continuously. The combined effect, however, does not always result in the desirable monotonicity in either variable. Because

$$\frac{df(\mathbf{x}(t), \mathbf{y}(t))}{dt} = \left\| \frac{\partial f}{\partial \mathbf{y}} \right\|^2 - \left\| \frac{\partial f}{\partial \mathbf{x}} \right\|^2$$

along a trajectory of (2.2), the objective values of f can either increase or decrease, depending on the sign of the difference between magnitudes of partial gradients along the trajectory which, in turn, depends on the starting point. Though the flow (2.2) may not conclusively vary the objective values in the way we prefer to see, it is still valid to say that the movement of $\mathbf{x}$ does not cause f to increase and $\mathbf{y}$ does not cause f to decrease.

One possible modification of (2.2) is to weight the vector fields of $\mathbf{x}$ and $\mathbf{y}$ differently, i.e.,

$$\begin{cases} \frac{d\mathbf{x}}{dt} &= -\alpha(t)\frac{\partial f}{\partial \mathbf{x}}, \\ \frac{d\mathbf{y}}{dt} &= \beta(t)\frac{\partial f}{\partial \mathbf{y}}, \end{cases} \tag{2.3}$$

where $\alpha(t)$ and $\beta(t)$ are positive scalars varying in time to provide a sense of controlled simulated annealing. For instance, by injecting a sufficiently large excitement from $\beta(t)$, we may be able to pull the flow $(\mathbf{x}(t), \mathbf{y}(t))$ out of a basin surrounding a local minimizer of f and let it go to somewhere else. Indeed, we may even allow $\beta(t)$ to be negative temporarily to introduce a descent flow and so on. In this way, the weight functions $\alpha(t)$ and $\beta(t)$ can be used as time-varying handles to steel the variation of $f(\mathbf{x}(t), \mathbf{y}(t))$. The real challenge is to derive an effective control strategy so that the weighted flow moves in the way we want it to be. We shall focus on the basic flow in this paper.

3. Relation to other flows. Before we further study properties of the maximin flow, it might be instructive to compare (2.2) with a few other dynamical systems of similar form.

3.1. Gradient flows. Gradient adaption is ubiquitous in nature and has been employed over a wide range of applications. Simply put, a dynamical system in the form

$$\frac{d\boldsymbol{\xi}}{dt} = -\nabla f(\boldsymbol{\xi}), \quad \boldsymbol{\xi}(0) = \boldsymbol{\xi}_0, \tag{3.1}$$

where f is a second-order differentiable functional of the variable $\boldsymbol{\xi}$ over an appropriately defined Hilbert space, is referred to as a (negative) gradient flow. Thermal conduction along the negative temperature gradient of the isothermal surfaces and osmosis down the concentration gradient across the cell membrane typify the gradient adaption in nature. A surprisingly large number of well-known diffusive partial differential equations have the intrinsic structure of a gradient flow with respect to some properly chosen energies and dissipative mechanisms [28]. Mathematical models for the phase separation of materials in iron alloys, the segmentation or edge detection in image processing or computer vision, the surface evolution in differential geometry, the flow of an ideal gas in porous medium, and the ground state in quantum systems all employ this notion of gradient flow [16]. Numerous other systems that evolve in time can also be interpreted as gradient dynamics, including applications in the game theory, financial markets, and mechanism design [4, 18, 22].

Assuming that the gradient flow takes place in a Euclidian space, we rewrite $\boldsymbol{\xi} = (\mathbf{x}, \mathbf{y}) \in \mathbb{R}^n \times \mathbb{R}^m$ and split the gradient flow (3.1) as the system

$$\begin{cases} \frac{d\mathbf{x}}{dt} &= -\frac{\partial f}{\partial \mathbf{x}}, \\ \frac{d\mathbf{y}}{dt} &= -\frac{\partial f}{\partial \mathbf{y}}. \end{cases} \tag{3.2}$$

for comparison with the maximin flow (2.2). The one sign difference makes a significant difference in several ways. The objective value of f along a maximin trajectory generally does not exhibit any monotonicity, but along a gradient trajectory the objective function $f(\boldsymbol{\xi}(t))$ is guaranteed to decrease to a (local) minimum. The maximin flow $(\mathbf{x}(t), \mathbf{y}(t))$ may wander off, if the index is incorrectly assumed or if the orientation is wrongly assigned. For gradient flow, the set of accumulation points

$$\omega(\boldsymbol{\xi}(0)) := \{\boldsymbol{\xi}^* \in \mathbb{R}^n \times \mathbb{R}^m \,|\, \boldsymbol{\xi}(t_\nu) \to \boldsymbol{\xi}^* \text{ for some sequence } t_\nu \to \infty\} \tag{3.3}$$

is a non-empty, compact, and connected subset of stationary points

$$\mathcal{C} := \{\boldsymbol{\xi} \in \mathbb{R}^n \times \mathbb{R}^m \,|\, \nabla f(\boldsymbol{\xi}) = 0\}. \tag{3.4}$$

If f is analytic, then $\omega(\boldsymbol{\xi}(0))$ is necessarily a singleton, implying the global convergence of $\boldsymbol{\xi}(t)$ [1, Theorem 1].

THEOREM 3.1. *Suppose that $f : U \to \mathbb{R}$ is real analytic in an open set $U \subset \mathbb{R}^n \times \mathbb{R}^m$. Then for any bounded semi-orbit of (3.2), there exists a point $\boldsymbol{\xi}^*$ such that $\boldsymbol{\xi}(t) \to \boldsymbol{\xi}^*$ as $t \to \infty$.*

3.2. Hamiltonian flows. In Hamiltonian mechanics, a classical physical system is described by a set of canonical coordinates $\mathbf{r} = (\mathbf{q}, \mathbf{p}) \in \mathbb{R}^n \times \mathbb{R}^n$, whereas the time evolution of the system is governed by Hamilton's equations

$$\left\{ \begin{array}{rcl} \frac{d\mathbf{p}}{dt} & = & -\frac{\partial \mathcal{H}}{\partial \mathbf{q}} \\ \frac{d\mathbf{q}}{dt} & = & +\frac{\partial \mathcal{H}}{\partial \mathbf{p}} \end{array} \right. \tag{3.5}$$

with $\mathcal{H} = \mathcal{H}(\mathbf{q}, \mathbf{p}, t)$ denoting the Hamiltonian which often corresponds to the total energy of the system. Typically, we can think of $\mathbf{q}$ as the space coordinate and $\mathbf{p}$ as the momentum. Then the first Hamilton equation can be interpreted as that the Newtonian force is equal to the negative gradient of the energy and the second equation as the velocity vector.

Renaming the function $\mathcal{H} \leftrightarrow f$ and the variables $\mathbf{p} \leftrightarrow \mathbf{x}$ and $\mathbf{q} \leftrightarrow \mathbf{y}$, we see a considerable similarity of the Hamiltonian flow (3.5) to the maximin flow (2.2) and the gradient flow (3.2). The main difference is at the symplectic structure of the Hamiltonian system, that is, by defining

$$\Omega = \left[\begin{array}{c|c} 0 & I_n \\ \hline -I_n & 0 \end{array} \right] \in \mathbb{R}^{2n \times 2n}, \tag{3.6}$$

the Hamiltonian equations can be expressed as

$$\left[\begin{array}{c} \frac{d\mathbf{x}}{dt} \\ \frac{d\mathbf{y}}{dt} \end{array} \right] = -\Omega \left[\begin{array}{c} \frac{\partial f}{\partial \mathbf{x}} \\ \frac{\partial f}{\partial \mathbf{y}} \end{array} \right]. \tag{3.7}$$

It follows easily that, if the Hamiltonian $\mathcal{H} \leftrightarrow f$ is not explicitly dependent on time, then $f(\mathbf{x}(t), \mathbf{y}(t))$ maintains constant along any integral curve of the Hamiltonian flow. Furthermore, if $\mathcal{H}$ is not constant itself over an open domain $U \in \mathbb{R}^n \times \mathbb{R}^n$, then the system (3.5) cannot have asymptotically stable equilibrium point in U.

3.3. Complex differential equations. Maximin flows do arise naturally in systems of complex-valued differential equations [3, 23]. This is mainly because a complex differentiable function at every point in a region is necessarily analytic on the region. Though these two types of flows are not equivalent, their interplay might help understand the classical ODE theory as well as the maximin flows.

Consider first the scalar case

$$\frac{dz}{dt} = -g'(z), \tag{3.8}$$

where $g(z)$ is a complex differentiable function in $z \in \mathbb{C}$. Write $z = x + \imath y$ and $g(z) = u(x, y) + \imath v(x, y)$ with $\imath = \sqrt{-1}$. Then $g'(z)$ must satisfy the Cauchy-Riemann equations

$$\left\{ \begin{array}{rcl} \frac{\partial u}{\partial x} & = & \frac{\partial v}{\partial y}, \\ \frac{\partial u}{\partial y} & = & -\frac{\partial v}{\partial x}. \end{array} \right.$$

In this case, it is known that

$$g'(z) = \frac{\partial u}{\partial x} - \imath \frac{\partial u}{\partial y} = \frac{\partial v}{\partial y} + \imath \frac{\partial v}{\partial x}.$$

Upon comparison of the real and the imaginary parts, we see that (3.8) is equivalent to

$$\left\{ \begin{array}{rcl} \frac{dx}{dt} & = & -\frac{\partial u}{\partial x}, \\ \frac{dy}{dt} & = & \frac{\partial u}{\partial y}, \end{array} \right. \tag{3.9}$$

which is precisely a $\max_y \min_x$ flow for the real-valued function $u(x, y)$. The well known monkey saddle $u(x, y) = x^3 - 3xy^2$, for example, is the real part of $g(z) = z^3$.

Conversely, suppose that a given function $u(x, y)$ is harmonic over a simply connected domain[1]. Then it is known that there exists a harmonic conjugate $v(x, y)$ such that the function $g(z) = u(x, y) + \imath v(x, y)$ is analytic [15]. The maximin flow (3.9) then is equivalent to the complex differential equation (3.8).

The forward argument above can be generalized to higher dimensions. The dynamical system

$$\frac{d\mathbf{z}}{dt} = -g'(\mathbf{z}), \tag{3.10}$$

where $g : \mathbb{C}^n \to \mathbb{C}$ is analytic, necessarily implies a $\max_{\mathbf{y}} \min_{\mathbf{x}}$ flow for the real part of g if we identify $\mathbf{z} = \mathbf{x} + \imath\mathbf{y}$ with $\mathbf{x}, \mathbf{y} \in \mathbb{R}^n$. Any property that is inherent to a maximin flow, therefore, holds for the complex flow $\mathbf{z}(t)$ solving (3.10). However, these two flows are not equivalent in high-dimensional domains. To check whether a given function $u : \mathbb{R}^n \times \mathbb{R}^m \to \mathbb{R}$ has a harmonic conjugate requires much more involvements. Being harmonic in each pair (x_i, y_i) of variables, where the derivative with respect to any extraneous variable is taken as zero if $m \neq n$, is not sufficient. We mention only in passing that for a multi-variable real-valued function $u(\mathbf{x}, \mathbf{y})$ to be the real part of a multi-variable complex-valued analytic function, it must be pluriharmonic, that is, u needs to satisfy the system of equations

$$\begin{cases} \frac{\partial u}{\partial x_\mu \partial x_\nu} + \frac{\partial u}{\partial y_\mu \partial y_\nu} &= 0 \\ \frac{\partial u}{\partial x_\mu \partial y_\nu} - \frac{\partial u}{\partial y_\mu \partial x_\nu} &= 0 \end{cases} \tag{3.11}$$

simultaneously for all μ and ν. While any complex ODE in $\mathbb{C}^n$ with analytic vector field automatically implies a maximin flow, only some special real-valued functions u can be pluriharmonic.

3.4. Minimum energy path. Rare but important transition events between long lived metastable states are a key feature of many systems arising in physics, chemistry, biology, and other fields. Finding the most probably transition pathway connecting local minima has been a long sought-after task. A suitable definition of a continuous line connecting reactants and products is still a subject of extensive investigation [21, 25, 29]. The idea of minimum energy path (MEP) is to construct a differential equation whose integral curve characterizes such a path. Suppose that a potential energy function $V : \mathbb{R}^n \to \mathbb{R}$ is given. One possible concept is that the MEP should be the path Γ such that each fixed point $\mathbf{w}_0 \in \Gamma$ assumes the minimum energy $V(\mathbf{w}_0)$ among all points on the hyperplane perpendicular to the path Γ at $\mathbf{w}_0$. Upholding this principle, the so called string method and its variants have already been proposed for computing this path [13, 30, 31]. We now argue that any path respecting this principle is actually a gradient flow.

To determine the MEP, we need to know its tangent vectors. To determine the tangent vector $\boldsymbol{\tau}(\mathbf{w}_0)$ of Γ at $\mathbf{w}_0$, we note that every point $\mathbf{w}$ on the hyperplane perpendicular to Γ at $\mathbf{w}_0$ can be uniquely expressed as

$$\mathbf{w} = \mathbf{w}_0 + B\mathbf{v},$$

where columns of $B = [\mathbf{b}_1, ..., \mathbf{b}_{n-1}]$ form a basis of the null space of $\boldsymbol{\tau}(\mathbf{w}_0)$ and $\mathbf{v}$ is arbitrary in $\mathbb{R}^{n-1}$. Define

$$G(\mathbf{v}; \mathbf{w}_0, \boldsymbol{\tau}) := V(\mathbf{w}_0 + B\mathbf{v})$$

Trivially, we see that

$$\nabla G(\mathbf{v}) = \nabla V(\mathbf{w}_0 + B\mathbf{v})B.$$

To attain minimum energy, necessarily we want $\nabla G = 0$ for some suitable $\mathbf{v}$. It follows that the gradient vector $\nabla V(\mathbf{w}_0 + B\mathbf{v})$ must be parallel to $\boldsymbol{\tau}(\mathbf{w}_0)$. In particular, at $\mathbf{w}_0$ where $\mathbf{v} = 0$, we see that the tangent vector $\boldsymbol{\tau}$ of Γ must be

$$\boldsymbol{\tau}(\mathbf{w}_0) = \pm\nabla V(\mathbf{w}_0). \tag{3.12}$$

[1]Recall the maximum principle that a harmonic function cannot have a local extreme within the domain of its definition. Thus any function u that exhibits a local maximum or minimum cannot be harmonic. Saddle points, if exist, is the only other option.

Note that the above argument makes no reference to what $\mathbf{w}_0$ should be. Starting from any given $\mathbf{w}_0$, we determine the direction $\boldsymbol{\tau}(\mathbf{w}_0)$ as is specified in (3.12). In other words, the so called string method for computing the minimum energy path between two local minima is in reality a gradient flow in itself. The choice of sign in (3.12) depends on whether we want to move up or down the hill.

3.5. Gradient flows in Kreĭn space. Given a complex linear space $\mathcal{K}$, a Hermitian sesquilinear form $[\![\cdot,\cdot]\!] : K \times K \to \mathbb{C}$ satisfying the linearity $[\![\alpha_1\mathbf{s}_1 + \alpha_2\mathbf{s}_2, \mathbf{t}]\!] = \alpha_1[\![\mathbf{s}_1,\mathbf{t}]\!] + \alpha_2[\![\mathbf{s}_2,\mathbf{t}]\!]$ and the conjugate symmetry $[\![\mathbf{s}_1,\mathbf{t}]\!] = \overline{[\![\mathbf{t},\mathbf{s}_1]\!]}$ for all $\mathbf{s}_1,\mathbf{s}_2,\mathbf{t} \in K$ and $\alpha_1,\alpha_2 \in \mathbb{C}$ is called an indefinite inner product over $\mathcal{K}$. If $\mathcal{K}$ is the direct sum of two subspaces

$$\mathcal{K} = \mathcal{K}_+ \oplus \mathcal{K}_- \tag{3.13}$$

such that $\mathcal{K}_+$ and $\mathcal{K}_-$ are Hilbert subspaces with respect to the inner product $[\![\cdot,\cdot]\!]$ and $-[\![\cdot,\cdot]\!]$, respectively, then $\mathcal{K}$ is called a Kreĭn space [6, 12, 14]. Any given $\mathbf{s},\mathbf{t} \in \mathcal{K}$ can be uniquely expressed as $\mathbf{s} = \mathbf{s}_+ + \mathbf{s}_-$ and $\mathbf{t} = \mathbf{t}_+ + \mathbf{t}_-$ with $\mathbf{s}_\pm, \mathbf{t}_\pm \in \mathcal{K}_\pm$. The bilinear form

$$\langle \mathbf{s},\mathbf{t}\rangle := [\![\mathbf{s}_+,\mathbf{t}_+]\!] - [\![\mathbf{s}_-,\mathbf{t}_-]\!] \tag{3.14}$$

defines a positive-definite inner product on $\mathcal{K}$. With respect to this inner product, the splitting (3.13) can be regarded as an orthogonal decomposition of $\mathcal{K}$. Let $\mathcal{P}_+$ and $\mathcal{P}_-$ denote the orthogonal projection onto $\mathcal{K}_+$ and $\mathcal{K}_-$, respectively. Then the operator $\mathcal{J}$ defined by

$$\mathcal{J} := \mathcal{P}_+ - \mathcal{P}_- \tag{3.15}$$

has the properties that $\mathcal{J}^3 = \mathcal{J}$, $\mathcal{J}^* = \mathcal{J}$, and $[\![\mathbf{s},\mathbf{t}]\!] = \langle \mathcal{J}\mathbf{s},\mathbf{t}\rangle$. The Minkowski space, for example, is a Kreĭv space with

$$\mathcal{J} = \begin{bmatrix} 1 & 0 & 0 & 0 \\ 0 & 1 & 0 & 0 \\ 0 & 0 & 1 & 0 \\ 0 & 0 & 0 & -1 \end{bmatrix}.$$

More generally, the space $\mathbb{R}^n \times \mathbb{R}^m$ equipped with the (indefinite) inner product

$$[\![(\mathbf{x}_1,\mathbf{y}_1),(\mathbf{x}_2,\mathbf{y}_2)]\!] := \mathbf{x}_1^\top\mathbf{x}_2 - \mathbf{y}_1^\top\mathbf{y}_2 \tag{3.16}$$

for $\mathbf{x}_i \in \mathbb{R}^n$ and $\mathbf{y}_i \in \mathbb{R}^m$, $i = 1, 2$, is a Kreĭn space.

It can be argued that the Riesz representation theorem continues to hold in a Kreĭv space [12, Page 147]. Therefore, the Fréchet derivative of a differentiable functional f over a Kreĭv space $\mathbb{R}^n \times \mathbb{R}^m$ has a vector representation with respect to the indefinite inner product (3.16). Specifically, there exists a pair of vectors $(\widehat{\mathbf{x}},\widehat{\mathbf{y}})$ such that

$$f'(\mathbf{x},\mathbf{y}).(\mathbf{h},\mathbf{k}) = [\![(\widehat{\mathbf{x}},\widehat{\mathbf{y}}),(\mathbf{h},\mathbf{k})]\!] \tag{3.17}$$

for all $(\mathbf{h},\mathbf{k}) \in \mathbb{R}^n \times \mathbb{R}^m$. In other words, with respect to the indefinite inner product, the "gradient" of f should be interpreted as the vector

$$\blacktriangledown f := \left(\frac{\partial f}{\partial \mathbf{x}}, -\frac{\partial f}{\partial \mathbf{y}}\right) = \mathcal{J}\nabla f$$

in the space $\mathbb{R}^n \times \mathbb{R}^m$. Therefore, the dynamical system (2.2), written as

$$\frac{d}{dt}\begin{bmatrix} \mathbf{x} \\ \mathbf{y} \end{bmatrix} = -\blacktriangledown f(\mathbf{x},\mathbf{y}), \tag{3.18}$$

can be regarded as a negative gradient flow in the Kreĭn space $\mathbb{R}^n \times \mathbb{R}^m$.

4. Properties of minimax flow. In contrast to the standard gradient flow and the Hamiltonian flow, we cannot draw any general conclusion about the global behavior of a maximin flow from (2.2). Still, under some mild assumptions, we can argue properties of local convergence and contractivity.

4.1. Local convergence. Consider the generic case that the maximin problem (2.1) has an isolate solution. Without of generality, assume that f has a saddle point at $(\mathbf{0},\mathbf{0})$ with $\nabla f(\mathbf{0},\mathbf{0})=0$ and an indefinite Hessian $H(\mathbf{0},\mathbf{0})$. We see that $(\mathbf{0},\mathbf{0})$ is also an equilibrium point for the differential system (2.2). In the way it is set up, we know a priori the orientation and the index of this saddle point — for a fixed $\mathbf{y}$ near the origin, $\mathbf{x}=0$ is a local minimizer and, for a fixed fixed $\mathbf{x}$, $\mathbf{y}=0$ is a local maximizer. Assume that the Hessian $H(\mathbf{0},\mathbf{0})$ is non-degenerate[2] in the sense that the maximin feature can be translated into the case that the two diagonal blocks

$$f_{\mathbf{xx}} := \frac{\partial^2 f}{\partial \mathbf{x}^2} = \left[\frac{\partial^2 f}{\partial x_i \partial x_j}\right] \in \mathbb{R}^{n\times n},$$
$$f_{\mathbf{yy}} := \frac{\partial^2 f}{\partial \mathbf{y}^2} = \left[\frac{\partial^2 f}{\partial y_s \partial y_t}\right] \in \mathbb{R}^{m\times m}$$

of $H(\mathbf{0},\mathbf{0})$ are positive and negative definite, respectively.

To understand the behavior of the differential system (2.2) near the equilibrium $(\mathbf{0},\mathbf{0})$, it suffices to consider the stability of its linearized system

$$\begin{bmatrix} \frac{d\mathbf{x}}{dt} \\ \frac{d\mathbf{y}}{dt} \end{bmatrix} = \underbrace{\begin{bmatrix} -\frac{\partial^2 f}{\partial \mathbf{x}\partial \mathbf{x}} & -\frac{\partial^2 f}{\partial \mathbf{y}\partial \mathbf{x}} \\ \frac{\partial^2 f}{\partial \mathbf{x}\partial \mathbf{y}} & \frac{\partial^2 f}{\partial \mathbf{y}\partial \mathbf{y}} \end{bmatrix}}_{J} \begin{bmatrix} \mathbf{x} \\ \mathbf{y} \end{bmatrix} \tag{4.1}$$

at the origin. For arbitrary $[\mathbf{u}^\top,\mathbf{v}^\top]^\top \in \mathbb{R}^n\times\mathbb{R}^m$, observe that

$$[\mathbf{u}^\top,\mathbf{v}^\top]J\begin{bmatrix}\mathbf{u}\\ \mathbf{v}\end{bmatrix} = -\mathbf{u}^\top f_{\mathbf{xx}}\mathbf{u} + \mathbf{v}^\top f_{\mathbf{yy}}\mathbf{v} < 0, \tag{4.2}$$

implying that the Jacobian matrix J is negative definite. Note that J is not symmetric in general. Still, all eigenvalues of J have negative real part[3].

LEMMA 4.1. *Suppose that $(\mathbf{x}^*,\mathbf{y}^*)$ is an isolate solution to the maximin problem (2.1) at which $f_{\mathbf{xx}}$ is positive definite and $f_{\mathbf{yy}}$ is positive definite. Then $(\mathbf{x}^*,\mathbf{y}^*)$ is an asymptotically stable equilibrium point for the maximin flow (2.2).*

We stress again that the dynamical system (2.2) is for the specific orientation $\max_{\mathbf{y}}\min_{\mathbf{x}}$ and for the specific index that the variable $\mathbf{x}\in\mathbb{R}^n$ represents. If a saddle point of f happens to have a different orientation or a different distribution of the index among the variables $\mathbf{x}$ and $\mathbf{y}$, and if we insist on using (2.2), then an argument similar to the above can prove that such a saddle point is a repeller. Using a similar argument, all other equilibria which are extreme points of f are necessarily repellers with respect to (2.2). If a saddle point is known to be of index one, its orientation, i.e., the negative eigenvector direction, can sometimes be estimated by sufficient sampling [27]. Determining the correct index and the associated orientation at a saddle point for a high-dimension problem in general is itself a challenging task.

4.2. Contractivity. The local convergence only explains how each individual trajectory is attracted to an asymptotically stable equilibrium point. We know argue that between two maximin flows a phenomenon of contraction is also taking place.

[2]For a degenerate case, see Examples 4 and 5 in Section 5. Sometimes local convergence can still be achieved using more sophisticated tools such as the central manifold theorem [9].

[3]Indeed, in many of the examples below, we see that the trajectories exhibit a spiral behavior, indicating the presence of imaginary part of eigenvalues.

4.2.1. Standard contraction. To avoid confusion, also for comparison, we first briefly review the notion of standard contraction [24, Chapter 7]. A vector field

$$\boldsymbol{\xi}' = \mathbf{f}(t, \boldsymbol{\xi}) \tag{4.3}$$

with $\mathbf{f} : D \subset [a, b] \times \mathbb{R}^n \to \mathbb{R}^n$ is said to satisfy a one-sided Lipschitz condition[4] if there exists a scalar function $\nu(t)$ such that the inequality

$$\langle \mathbf{f}(t, \boldsymbol{\xi}_1) - \mathbf{f}(t, \boldsymbol{\xi}_2), \boldsymbol{\xi}_1 - \boldsymbol{\xi}_2 \rangle \leq \nu(t) \|\boldsymbol{\xi}_1 - \boldsymbol{\xi}_2\|_2^2 \tag{4.4}$$

holds for all $\boldsymbol{\xi}_1, \boldsymbol{\xi}_2$ in the set $\{\boldsymbol{\xi} \in \mathbb{R}^n | (t, \boldsymbol{\xi}) \in D\}$. The one-sided Lipschitz function $\nu(t)$ in (4.4) can be negative. Suppose that $\boldsymbol{\xi}(t)$ and $\boldsymbol{\zeta}(t)$ are two solutions of (4.3). Then it can be argued that [24, Section 7.3] (see also [17, Lemma 12.1])

$$\|\boldsymbol{\xi}(t_2) - \boldsymbol{\zeta}(t_2)\|_2 \leq e^{\int_{t_1}^{t_2} \nu(\xi) d\xi} \|\boldsymbol{\xi}(t_1) - \boldsymbol{\zeta}(t_1)\|_2, \quad a \leq t_1 \leq t_2 \leq b. \tag{4.5}$$

A contraction happens (segmentally) over the interval $[a, b]$ when $e^{\int_{t_1}^{t_2} \nu(\xi) d\xi} < 1$ for $a \leq t_1 \leq t_2 \leq b$. This has been used as an effective tool for studying the nonlinear stability. For gradient dynamics (3.1), we take the autonomous system

$$\mathbf{f}(t, \boldsymbol{\xi}) = \mathbf{f}(\boldsymbol{\xi}) := -\nabla f(\boldsymbol{\xi}). \tag{4.6}$$

The following lemma shows that at regions where f displays a local convexity the flows enjoy contractivity [10, Lemma 2.1].

LEMMA 4.2. *Suppose that the objection function f is second-order continuously differentiable over a neighborhood of $\widehat{\boldsymbol{\xi}}$ and that $\nabla^2 f(\widehat{\boldsymbol{\xi}})$ is positive definite. Then there is a closed ball $\mathcal{B} = \mathcal{B}(\widehat{\boldsymbol{\xi}})$ centered at $\widehat{\boldsymbol{\xi}}$ and a positive number $\lambda_{\mathcal{B}}$ such that*

$$\langle -\nabla f(\boldsymbol{\xi}_1) + \nabla f(\boldsymbol{\xi}_2), \boldsymbol{\xi}_1 - \boldsymbol{\xi}_2 \rangle = -\lambda_{\mathcal{B}} \|\boldsymbol{\xi}_1 - \boldsymbol{\xi}_2\|_2^2 \tag{4.7}$$

for any $\boldsymbol{\xi}_1, \boldsymbol{\xi}_2 \in \mathcal{B}$. The gradient flow is contractive in the sense

$$\|\boldsymbol{\xi}(t_2) - \boldsymbol{\zeta}(t_2)\|_2 \leq e^{-(t_2 - t_1)\lambda_{\mathcal{B}}} \|\boldsymbol{\xi}(t_1) - \boldsymbol{\zeta}(t_1)\|_2, \quad a \leq t_1 \leq t_2 \leq b \tag{4.8}$$

between any two gradient flows $\boldsymbol{\xi}(t)$ and $\boldsymbol{\zeta}(t)$ with starting points in $\mathcal{B}$.

We stress that the phenomenon of contractivity is region dependent. In particular, the exponential rate $\lambda_{\mathcal{B}}$ of contraction varies from region to region.

4.2.2. Contraction in Kreĭn space. For our application, we work in the Kreĭn space $\mathbb{R}^n \times \mathbb{R}^m$ equipped with the indefinite inner product (3.16). Mimicking the Minkowski metric, we introduce the notation

$$\|\!|\boldsymbol{\xi}|\!\|^2 = [\![\boldsymbol{\xi}, \boldsymbol{\xi}]\!] = \langle \mathbf{x}, \mathbf{x} \rangle - \langle \mathbf{y}, \mathbf{y} \rangle \tag{4.9}$$

for $\boldsymbol{\xi} = (\mathbf{x}, \mathbf{y}) \in \mathbb{R}^n \times \mathbb{R}^m$. Note that $\|\!| \cdot |\!\|$ is not a norm and that the quantity $\|\!|\boldsymbol{\xi}|\!\|^2$ may be negative. For maximin flows (2.2), we have

$$\mathbf{f}(t, \boldsymbol{\xi}) = \mathbf{f}(\boldsymbol{\xi}) = -\blacktriangledown f(\boldsymbol{\xi}) := \begin{bmatrix} -\nabla_{\mathbf{x}} f(\mathbf{x}, \mathbf{y}) \\ \nabla_{\mathbf{y}} f(\mathbf{x}, \mathbf{y}) \end{bmatrix}. \tag{4.10}$$

Under the same conditions as in Lemma 4.2, for $\boldsymbol{\xi}_1, \boldsymbol{\xi}_2$ nearby a point $\widehat{\boldsymbol{\xi}}$ where $\nabla^2 f(\widehat{\boldsymbol{\xi}})$ is positive definite, observe that

$$\begin{aligned} [\![-\blacktriangledown f(\boldsymbol{\xi}_1) + \blacktriangledown f(\boldsymbol{\xi}_2), \boldsymbol{\xi}_1 - \boldsymbol{\xi}_2]\!] &= \langle -\nabla_{\mathbf{x}} f(\boldsymbol{\xi}_1) + \nabla_{\mathbf{x}} f(\boldsymbol{\xi}_2), \boldsymbol{x}_1 - \boldsymbol{x}_2 \rangle - \langle \nabla_{\mathbf{x}} f(\boldsymbol{\xi}_1) - \nabla_{\mathbf{x}} f(\boldsymbol{\xi}_2), \boldsymbol{y}_1 - \boldsymbol{y}_2 \rangle \\ &= \langle -\nabla f(\boldsymbol{\xi}_1) + \nabla f(\boldsymbol{\xi}_2), \boldsymbol{\xi}_1 - \boldsymbol{\xi}_2 \rangle \leq -\lambda_{\mathcal{B}} \|\!|\boldsymbol{\xi}_1 - \boldsymbol{\xi}_2|\!\|^2, \end{aligned} \tag{4.11}$$

[4] A conventional Lipschitz condition necessarily implies a one-sided Lipschitz condition, but not the converse.

where the last inequality is due to the fact that

$$\|\boldsymbol{\xi}\|_2^2 \geq \|\!|\boldsymbol{\xi}|\!\|^2 \tag{4.12}$$

for any $\boldsymbol{\xi} \in \mathbb{R}^n \times \mathbb{R}^m$.

Suppose that $\boldsymbol{\xi}(t)$ and $\boldsymbol{\zeta}(t)$ are two saddle point flows with starting points in $\mathcal{B}$. Define the scalar function

$$\Omega(t) := \|\!|\boldsymbol{\xi}(t) - \boldsymbol{\zeta}(t)|\!\|^2. \tag{4.13}$$

Then by the linearity and conjugate symmetry of the inner product over real numbers, we have

$$\frac{d\Omega}{dt} = 2\left[\!\!\left[\frac{d\boldsymbol{\xi}}{dt} - \frac{d\boldsymbol{\zeta}}{dt}, \boldsymbol{\xi}(t) - \boldsymbol{\zeta}(t)\right]\!\!\right] = 2[\![-\blacktriangledown f(\boldsymbol{\xi}_1) + \blacktriangledown f(\boldsymbol{\xi}_2), \boldsymbol{\xi}_1 - \boldsymbol{\xi}_2]\!] \leq -2\lambda_{\mathcal{B}}\Omega(t), \tag{4.14}$$

where the inequality follows from (4.11). Define the integrating factor $\omega(t) = e^{2\lambda_{\mathcal{B}} t}$ which is always positive, we find that

$$\frac{d(\omega(t)\Omega(t))}{dt} \leq 0 \tag{4.15}$$

whenever $\Omega(t)$ is defined. In particular, we see the contraction of the maximin flows in the following sense.

LEMMA 4.3. *Suppose that the objection function f is second-order continuously differentiable over a neighborhood of $\widehat{\boldsymbol{\xi}}$ and that $\nabla^2 f(\widehat{\boldsymbol{\xi}})$ is positive definite. Then there is a closed ball $\mathcal{B} = \mathcal{B}(\widehat{\boldsymbol{\xi}})$ centered at $\widehat{\boldsymbol{\xi}}$ and a positive number $\lambda_{\mathcal{B}}$ such that*

$$\|\!|\boldsymbol{\xi}(t_2) - \boldsymbol{\zeta}(t_2)|\!\|^2 \leq e^{-2\lambda_B(t_2-t_1)}\|\!|\boldsymbol{\xi}(t_1) - \boldsymbol{\zeta}(t_1)|\!\|^2, \tag{4.16}$$

between any two gradient flows $\boldsymbol{\xi}(t)$ and $\boldsymbol{\zeta}(t)$ with starting points in $\mathcal{B}$ and $t_1 < t_2$.

The above result is interesting in its formality, but it measures only $\|\!|\boldsymbol{\xi}(t) - \boldsymbol{\zeta}(t)|\!\|^2$ which does not tell whether the two flows $\boldsymbol{\xi}(t)$ and $\boldsymbol{\zeta}(t)$ actually get closer or not. The proof also relies on the local convexity which certainly does not hold near a saddle point. Nevertheless, in the neighborhood of a saddle point we have already shown the asymptotic stability in Lemma 4.1.

4.3. Isolation. *Want to prove that the accumulating points, if exist, are isolated when f is analytic ... something similar to the Łojasiewicz gradient inequality.*

5. Examples. The followings examples are simple enough that we can precisely locate their saddle points and the associated orientations, but they might help to illuminate the interesting dynamics of (2.2). In particular, we want to demonstrate that following the flow often can lead to a saddle point without any a priori knowledge.

5.1. 3-D landscape and flow dynamics. We first consider a few nontrivial surfaces in $\mathbb{R}^3$ and demonstrate the corresponding dynamics by drawing sufficiently many of their trajectories. Of particular interest in these examples is the basin of attraction for each of the saddle points.

Example 1. The Müller-Brown potential energy surface

$$\begin{aligned} f(x,y) = &-200e^{-(x-1)^2-10y^2} - 100e^{-x^2-10(y-0.5)^2} \\ &-170e^{-6.5(x+0.5)^2+11(x+0.5)(y-1.5)-6.5(y-1.5)^2} + 15e^{0.7(x+1)^2+0.6(x+1)(y-1)+0.7(y-1)^2}. \end{aligned} \tag{5.1}$$

is a well studied surface which has three local minima and two saddle points, as can be seen from the drawings in Figure 5.1. From the plot, it is seen that the saddle point A is more in the $\max_{\mathbf{x}} \min_{\mathbf{y}}$ orientation, whereas the maximin property of B is less clear. Applying (2.2) to this potential function, we illustrate the dynamics by some trajectories in Figure 5.2, where from any given point the forward time integration produces a red curve and the backward time integration produces a black curve.

It is then observed that, since the orientation of the saddle point A is the opposite to that of problem (2.1), it is backward asymptotically stable for the differential system (2.2). The orientation of the point B is ambiguous.

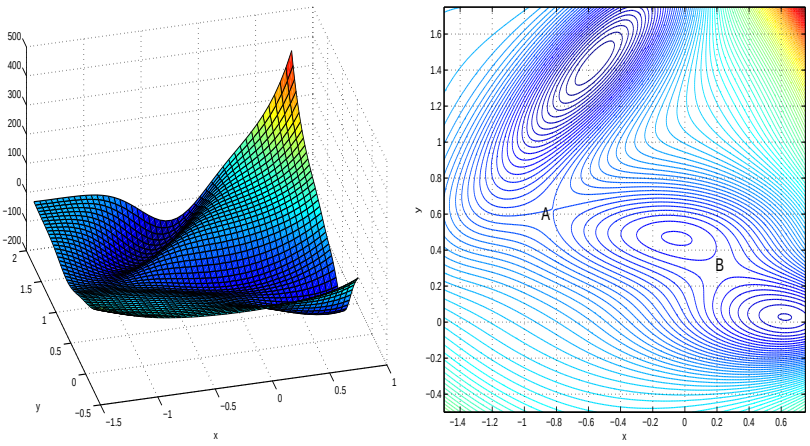

FIGURE 5.1. *Müller-Brown potential energy surface and level curves.*

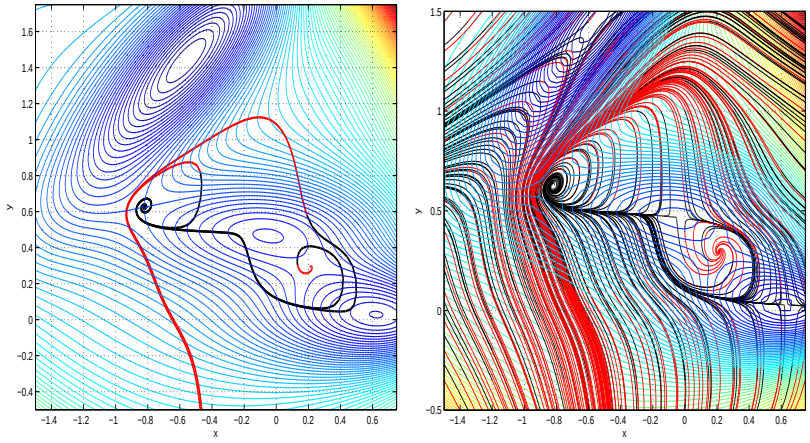

FIGURE 5.2. *Dynamics of (2.2) applied to the Müller-Brown potential energy surface (5.1). (red = forward time; black = backward time)*

It is proven numerically to be forward asymptotically stable, but its basin of attraction is considerably smaller than that of the point A. We note that all three local minima are repelling the flow away from them.

Example 2. The peak function used in MATLAB

$$f(x,y) = 3(1-x)^2 e^{-x^2-(y+1)^2} - 10(\frac{x}{5} - x^3 - y^5)e^{-x^2-y^2} - \frac{1}{3}e^{-(x+1)^2-y^2} \tag{5.2}$$

has three maxima, two minima, and three saddle points. The surface and the corresponding dynamics of (2.2) are plotted in Figure 5.3. The orientations of the saddle points are quite clear — only the gorge between the two south (negative y-axis) hills has the orientation $\max_{\mathbf{y}} \min_{\mathbf{x}}$, so it is forward asymptotically stable; the other two saddle points are backward asymptotically stable.

5.2. Singularity. We then demonstrate that near a singular point of a surface, the dynamics of the corresponding (2.2) could make abrupt changes due to discontinuity.

Example 3. The function

$$f(x,y) = (1-x^2-y^2)^2 + \frac{y^2}{x^2+y^2} \tag{5.3}$$

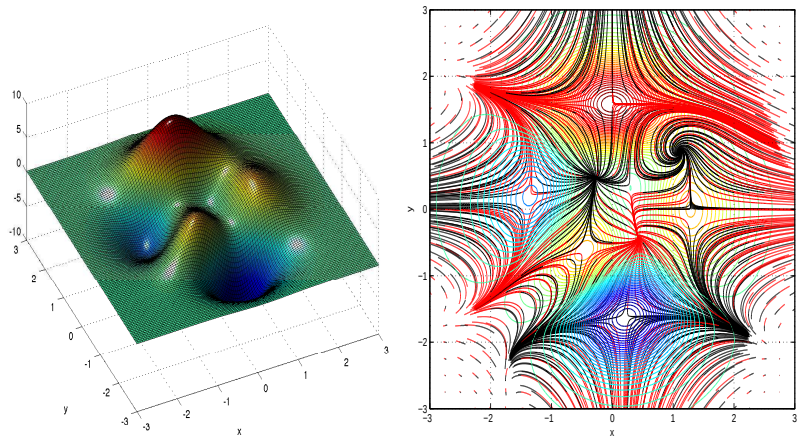

FIGURE 5.3. *Landscape and dynamics of (2.2) applied to the peak function (5.2). (red = forward time; black = backward time)*

is not defined at $(0, 0)$. The discontinuity at this point creates a topography that repels nearby forward flows (except those moving exactly along the ridge of $x = 0$) away from this crevasse. Note that this point is not backward asymptotically stable either, since flows on the ridge of $x = 0$ moves toward it. See Figure 5.4. The two real saddle points of f have orientation $\max_{\mathbf{x}} \min_{\mathbf{y}}$, so they are backward asymptotically stable.

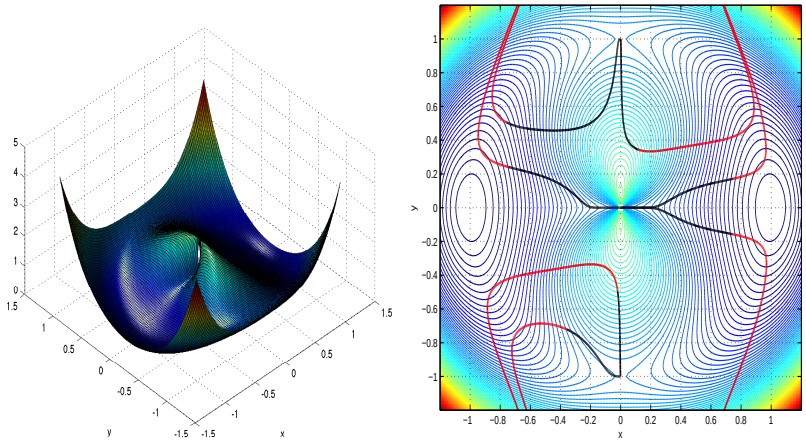

FIGURE 5.4. *Landscape and sample flows of (2.2) applied to the function (5.3) with a pole at* $(0, 0)$. *(red = forward time; black = backward time)*

5.3. Degenerate Hessian. The following two examples demonstrate two distinct scenarios when the Hessian of f is degenerate.

Example 4. Consider the linear programming problem

$$\mathcal{P}_L : \begin{cases} \text{minimize} & \mathbf{c}^\top \mathbf{x}, \\ \text{subject to} & A\mathbf{x} = \mathbf{b}, \end{cases}$$

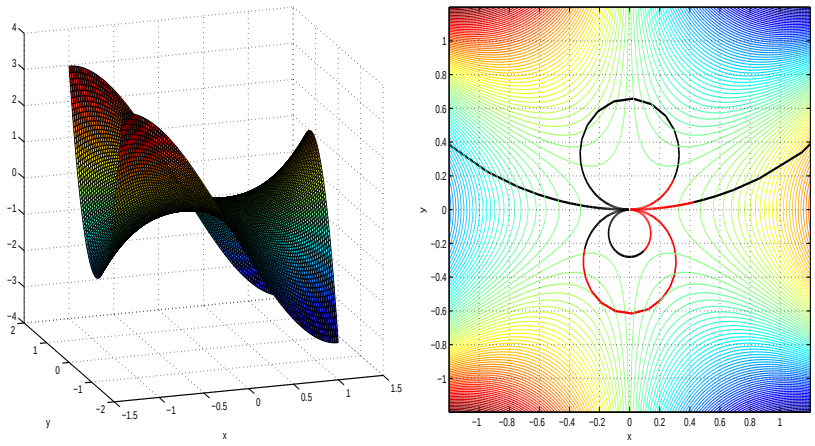

FIGURE 5.5. *Landscape and dynamics of (2.2) applied to the monkey saddle function (5.4). (red = forward time; black = backward time)*

where, for simplicity, we assume that all inactive constraints have been ruled out[5]. Then the Hessian of the Lagrangian has the form

$$H = \begin{bmatrix} 0 & A^\top \\ A & 0 \end{bmatrix}$$

at every $(\mathbf{x}, \mathbf{y})$, which is degenerate in the sense that $f_{\mathbf{xx}} = 0$ and $f_{\mathbf{yy}} = 0$. So the argument for local convergence in the preceding section cannot be applied. Indeed, though the saddle point theorem still holds in this case, the differential equations (2.2) becomes

$$\frac{d}{dt}\begin{bmatrix} \mathbf{x} \\ \mathbf{y} \end{bmatrix} = \begin{bmatrix} 0 & -A^\top \\ A & 0 \end{bmatrix}\begin{bmatrix} \mathbf{x} \\ \mathbf{y} \end{bmatrix} - \begin{bmatrix} \mathbf{c} \\ \mathbf{b} \end{bmatrix}$$

which is a linear system with constant coefficients. We can easily write down its solution $(\mathbf{x}(t), \mathbf{y}(t))$ in closed form via the variation of constants formula. In particular, the solution to the problem $\mathcal{P}_L$ is not an asymptotically stable equilibrium for the dynamical system. Rather, it is a center. This is an example where the maximin flow fails. Fortunately, the saddle point is easy to find in this case.

Example 5. In contrast to Example 4, the Hessian at the monkey saddle point corresponding to the function

$$f(x, y) = x^3 - 3xy^2 \tag{5.4}$$

is also degenerated. Indeed, it is identically zero. However, it can easily be checked that the maximin flow is equivalent to the complex differential equation $\frac{dz}{dt} = -z^2$ which has a closed-form solution[6]. In this case, we can continue to argue the asymptotical stability which is in accordance with the one demonstrated in the right drawing of Figure 5.5

5.4. High-indexed saddle point. Saddle points at which the associated Hessian has more than one eigenvalues with negative real part are generally more challenging. Most of the discussions in the literature are for saddle points with index one [20, 30].

Example 6. Consider the higher dimensional function

$$w = f(x, y_1, y_2) = x^2 - y_1^2 - y_2^2 + x^3 - 3xy_1^2 - 3xy_2^2 - 3y_1y_2^2 \tag{5.5}$$

[5]Obviously, finding the active constraints is one of the main tasks in linear programming. Here we only want to demonstrate the degeneracy of the Hessian.

[6]We could also apply the central manifold theorem to the nonlinear portion of the corresponding dynamical system as well.

which has an index-2 saddle point at $(0,0,0)$ and an index-1 saddle point at $(-\frac{2}{3},0,0)$ with functional values 0 and $\frac{4}{27}$, respectively. Analogous to the three dimensional hyperbolic paraboloid, the "w-level surfaces" of the function (5.5) changes its phrase when passing through these saddle points. See Figure 5.6. To help see the

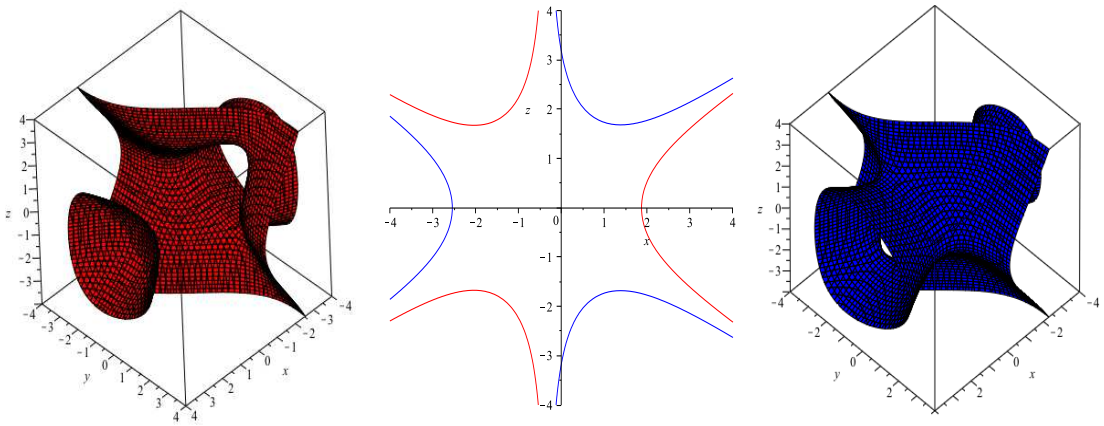

FIGURE 5.6. *Phase change of level surfaces of (5.5) at $w = 10$ (left) and $w = -10$ (right).*

anatomy of the surface better, we also dissect the level surface by the coronal plane $y_1 = 0$ and show the two different phases in the middle drawing of Figure 5.6.

What is most significant in this example is that, since there are two saddle points, there is a window of transition between $w = 0$ and $w = \frac{4}{27}$. We plot the cross sections of the two critical states in the left drawing of Figure 5.7. These critical states serve as the "asymptotes" of all level surfaces. Also plotted is one of the transition states before the phase change shown in Figure 5.6 emerges.

Before the above analysis is possible, it is crucial to first determinate the number and locations of saddle points. What is relevant to this paper is that we find the two saddle points by using our flow approach without first analyzing the derivative information. Two solution trajectories, starting with randomly selected initial points, are demonstrated in the right drawing of Figure 5.7, which shows that the saddle point $(0,0,0)$ is forward asymptotical stable, whereas the other saddle point $(-\frac{2}{3},0,0)$ is backward asymptotical stable.

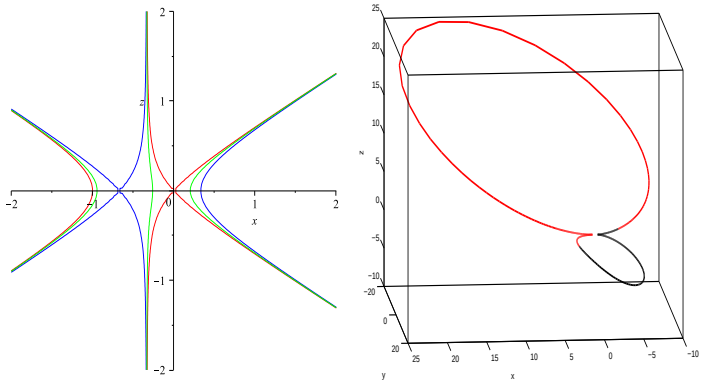

FIGURE 5.7. *Left: (Cross sections of) critical states at $w = \frac{4}{27}$ (blue) and $w = 0$ (red), and a transition state at $w = 0.05$ (green). Right: A solution trajectory for the system (2.2) applied to (5.5).*

[1] P.-A. ABSIL, R. MAHONY, AND R. SEPULCHRE, *Optimization algorithms on matrix manifolds*, Princeton University Press, Princeton, NJ, 2008.

[2] K. J. ARROW, L. HURWICZ, AND H. UZAWA, *Studies in linear and non-linear programming*, With contributions by H. B. Chenery, S. M. Johnson, S. Karlin, T. Marschak, R. M. Solow. Stanford Mathematical Studies in the Social Sciences, vol. II, Stanford University Press, Stanford, Calif., 1958.

[3] P. R. BEESACK, *On an existence theorem for complex-valued differential equations*, The American Mathematical Monthly, 65 (1958), pp. pp. 112–115.

[4] W. BEHRMAN, *An efficient gradient flow method for unconstrained optimization*, PhD thesis, Stanford University, 1998.

[5] A. BLOCH, R. BROCKETT, AND T. RATIU, *On the geometry of saddle point algorithms*, in Decision and Control, 1992., Proceedings of the 31st IEEE Conference on, 1992, pp. 1482–1487 vol.2.

[6] J. BOGNÁR, *Indefinite inner product spaces*, Springer-Verlag, New York-Heidelberg, 1974. Ergebnisse der Mathematik und ihrer Grenzgebiete, Band 78.

[7] S. BOYD AND L. VANDENBERGHE, *Convex optimization*, Cambridge University Press, Cambridge, 2004.

[8] M. CAMERON, R. V. KOHN, AND E. VANDEN-EIJNDEN, *The string method as a dynamical system*, J. Nonlinear Sci., 21 (2011), pp. 193–230.

[9] J. CARR, *Applications of centre manifold theory*, vol. 35 of Applied Mathematical Sciences, Springer-Verlag, New York, 1981.

[10] M. T. CHU, *Numerical methods for gradient dynamics*, preprint, North Carolina State University, 2016.

[11] I. CLEJAN, *A saddle point finding algorithm for functionals*, Computer Physics Communications, 77 (1993), pp. 57 – 63.

[12] M. A. DRITSCHEL AND J. ROVNYAK, *Operators on indefinite inner product spaces*, in Lectures on operator theory and its applications (Waterloo, ON, 1994), vol. 3 of Fields Inst. Monogr., Amer. Math. Soc., Providence, RI, 1996, pp. 141–232.

[13] W. E, W. REN, AND E. VANDEN-EIJNDEN, *Simplified and improved string method for computing the minimum energy paths in barrier-crossing events*, J. Chemical Physics, 126 (2007). `http://dx.doi.org/10.1063/1.2720838`.

[14] I. GOHBERG, P. LANCASTER, AND L. RODMAN, *Matrices and indefinite scalar products*, vol. 8 of Operator Theory: Advances and Applications, Birkhäuser Verlag, Basel, 1983.

[15] J. D. GRAY AND S. A. MORRIS, *When is a function that satisfies the Cauchy-Riemann equations analytic?*, Amer. Math. Monthly, 85 (1978), pp. 246–256.

[16] E. HAIRER AND C. LUBICH, *Energy-diminishing integration of gradient systems*, IMA J. Numer. Anal., 34 (2014), pp. 452–461.

[17] E. HAIRER AND G. WANNER, *Solving ordinary differential equations. II*, vol. 14 of Springer Series in Computational Mathematics, Springer-Verlag, Berlin, second ed., 1996. Stiff and differential-algebraic problems.

[18] J. K. HALE, *Asymptotic behavior off dissipative systems*, vol. 25 of Mathematical Surveys and Monographs, American Mathematical Society, Providence, RI, 1988.

[19] P. HÄNGGI, P. TALKNER, AND M. BORKOVEC, *Reaction-rate theory: fifty years after kramers*, Rev. Modern Physics, 62 (1990), p. 251.

[20] D. HEIDRICH AND W. QUAPP, *Saddle points of index 2 on potential energy surfaces and their role in theoretical reactivity investigations*, Theoretica chimica acta, 70 (1986), pp. 89–98.

[21] G. HENKELMAN, G. JÓHANNESSON, AND H. JÓNSSON, *Methods for finding saddle points and minimum energy paths*, Progress on Theoretical Chemistry and Physics, Kluwer Academic, 2006, ch. 10, pp. 269–302.

[22] M. W. HIRSCH AND S. SMALE, *Differential equations, dynamical systems, and linear algebra*, Academic Press [A subsidiary of Harcourt Brace Jovanovich, Publishers], New York-London, 1974. Pure and Applied Mathematics, Vol. 60.

[23] E. L. INCE, *Ordinary Differential Equations*, Dover Publications, New York, 1944.

[24] J. D. LAMBERT, *Numerical methods for ordinary differential systems*, John Wiley & Sons, Ltd., Chichester, 1991. The initial value problem.

[25] P. METZNER, C. SCHÃ?TTE, AND E. VANDEN-EIJNDEN, *Illustration of transition path theory on a collection of simple examples*, The Journal of Chemical Physics, 125 (2006).

[26] J. NOCEDAL AND S. J. WRIGHT, *Numerical optimization*, Springer Series in Operations Research and Financial Engineering, Springer, New York, second ed., 2006.

[27] A. PEDERSEN, S. F. HAFSTEIN, AND H. JÓNSSON, *Efficient sampling of saddle points with the minimum-mode following method*, SIAM J. Sci. Comput., 33 (2011), pp. 633–652.

[28] M. A. PELETIER, *Energies, gradient flows, and large deviations: a modelling point of view*, Lecture notes, Technische Universiteit Eindhoven, 2012. http://www.win.tue.nl/ mpeletie/Onderwijs/Pisa2011/PeletierLectureNotesPisa2011.pdf.

[29] W. QUAPP AND D. HEIDRICH, *Analysis of the concept of minimum energy path on the potential energy surface of chemically reacting systems*, Theoretica chimica acta, 66 (1984), pp. 245–260.

[30] W.-Q. REN, *Higher order string method for finding minimum energy paths*, Commun. Math. Sci., 1 (2003), pp. 377–384.

[31] A. SAMANTA AND W. E, *Optimization-based string method for finding minimum energy path*, Commun. Comput. Phys., 14 (2013), pp. 265–275.